

Time-Resolved X-ray Scattering of an Electronically Excited State in Solution. Structure of the $^3A_{2u}$ State of Tetrakis- μ -pyrophosphitodiplatinate(II)

Morten Christensen,[†] Kristoffer Haldrup,[†] Klaus Bechgaard,[†] Robert Feidenhans'l,[†] Qingyu Kong,^{‡,§} Marco Cammarata,^{†,‡} Manuela Lo Russo,[‡] Michael Wulff,[‡] Niels Harrit,^{*,†} and Martin Meedom Nielsen^{*,†}

Centre for Molecular Movies, Department of Chemistry and Niels Bohr Institute, University of Copenhagen, Universitetsparken 5, DK-2100 Copenhagen, Denmark, and The European Synchrotron Radiation Facility, BP220, Grenoble Cedex 38043, France

Received June 12, 2008; E-mail: harrit@fys.ku.dk

Abstract: The structure of the $^3A_{2u}$ excited state of tetrakis- μ -pyrophosphitodiplatinate(II) in aqueous solution is investigated by time-resolved X-ray scattering on a time scale from 100 ps to 1 μ s after optical pumping. The primary structural parameter, the Pt–Pt distance, is found to be 2.74 Å, which is 0.24 Å shorter than the ground-state value. The contraction is in excellent agreement with earlier estimates based on spectroscopic data in solution and diffraction data in the crystalline state. As a second structural parameter, the distance between the P planes in the $^3A_{2u}$ excited state was determined to be 2.93 Å, i.e., the same as that in the ground state. This result implies that a slight lengthening of the Pt–P bond occurs following excitation.

Introduction

Detailed knowledge of the structure of transient molecular species in solution is important to understand reaction pathways and dynamics. Addressing such details by X-ray scattering methods is hampered by the lack of coherent amplification of the signal normally provided by molecules arranged in crystal lattices and by the inherent short-lived nature of the transient species. However, the subnanosecond time resolution and high brilliance available at third-generation synchrotrons may overcome these difficulties. This is demonstrated in the present paper by an accurate determination of bonding distances in an electronically excited molecule in solution. The bonding distances obtained are distinctly different from similar data obtained from single-crystal experiments, showing the necessity of solution experiments.

Recent examples of time-resolved X-ray scattering (TRXRS) experiments in solution are the photolysis of HgI_2^1 and the successful determination of the interatomic distance in the A/A' state of molecular iodine dissolved in $CH_2Cl_2^2$ and CCl_4^3 . The population of A/A' states was predominantly formed as a transient species when iodine atoms recombined after photodissociation, less as a direct consequence of electronic excitation. Also, the structures of fragments and iodine-bridged species,

generated through recombination of photodissociated $CH_2I_2^4$, $C_2H_4I_2^5$, CHI_3^6 and $C_2F_4I_2^7$ in methanol, have been investigated and resolved.

In all the examples cited, iodine has served as a heavy nucleus to ensure sufficient scattering. With the intention to widen the scope and applicability of TRXRS methods in solution chemistry, the molecule of tetrakis- μ -pyrophosphitodiplatinate(II) ($Pt_2(P_2O_5H_2)_4^{4-}$, PtPOP)⁸ was selected as an ideal target in the present investigation due to its scattering power and its interesting photophysical and photochemical properties.^{9–11}

PtPOP has D_{4h} symmetry¹² with a square planar configuration around the two platinum atoms (Figure 1a). As in other binuclear d^8 complexes¹⁰ the lowest electronic energy transition is $5d\sigma^* \rightarrow 6p\sigma$, which results in a large contraction along the metal–metal coordinate.¹¹

- (4) Davidsson, J.; Poulsen, J.; Cammarata, M.; Georgiou, P.; Wouts, R.; Katona, G.; Jacobson, F.; Plech, A.; Wulff, M.; Nyman, G.; Neutze, R. *Phys. Rev. Lett.* **2005**, *94*, 245503.
- (5) Ihee, H.; Lorenc, M.; Kim, T. K.; Kong, Q. Y.; Cammarata, M.; Lee, J. H.; Bratos, S.; Wulff, M. *Science (Washington, D.C.)* **2005**, *309*, 1223.
- (6) Lee, J. H.; Kim, J.; Cammarata, M.; Kong, Q.; Kim, K. H.; Choi, J.; Kim, T. K.; Wulff, M.; Ihee, H. *Angew. Chem., Int. Ed.* **2008**, *47*, 1047.
- (7) Lee, J. H.; Kim, T. K.; Kim, J.; Kong, Q.; Cammarata, M.; Lorenc, M.; Wulff, M.; Ihee, H. *J. Am. Chem. Soc.* **2008**, *130*, 5834.
- (8) Sperline, R. P.; Dickson, M. K.; Roundhill, D. M. *J. C. S. Chem. Commun.* **1977**, 1977, 62.
- (9) Roundhill, D. M.; Gray, H. B.; Che, C. M. *Acc. Chem. Res.* **1989**, *22*, 55.
- (10) Smith, D. C.; Gray, H. B. *Coord. Chem. Rev.* **1990**, *100*, 169.
- (11) Zipp, A. P. *Coord. Chem. Rev.* **1988**, *84*, 47.
- (12) Dos Remedios Pinto, M. A. F.; Sadler, P. J.; Neidle, S.; Sanderson, M. R.; Subbiah, A.; Kuroda, R. *Chem. Commun.* **1980**, 13.

[†] University of Copenhagen.

[‡] The European Synchrotron Radiation Facility.

[§] Current address: Société civile Synchrotron SOLEIL, L'Orme des Merisiers, Saint-Aubin, BP 48, 91192 Gif-sur-Yvette Cedex, France.

- (1) Geis, A.; Bouriau, M.; Plech, A.; Schotte, F.; Techert, S.; Trommsdorff, H. P.; Wulff, M.; Block, D. *J. Lumin.* **2001**, *94*, 95, 493.
- (2) Neutze, R.; Wouts, R.; Techert, S.; Davidsson, J.; Kocsis, M.; Kirrander, A.; Schotte, F.; Wulff, M. *Phys. Rev. Lett.* **2001**, *87*, 195508.
- (3) Wulff, M.; Bratos, S.; Plech, A.; Vuilleumier, R.; Mirloup, F.; Lorenc, M.; Kong, Q.; Ihee, H. *J. Chem. Phys.* **2006**, *124*, 34501.

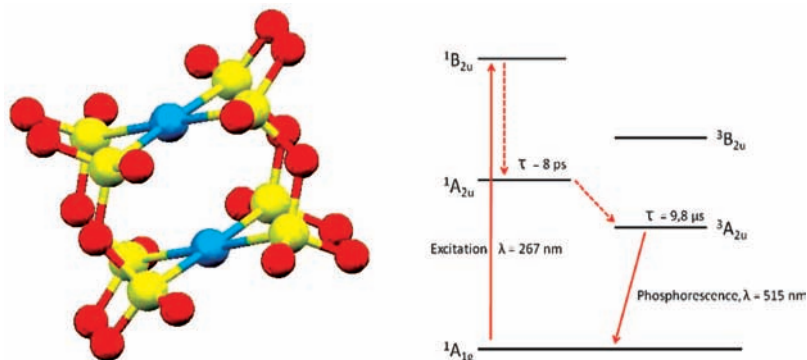


Figure 1. (a, left) Model structure of the PtPOP anion, $\text{Pt}_2(\text{P}_2\text{O}_5\text{H}_2)_4^{4-}$, without hydrogen atoms (Pt, blue; P, yellow; O, red). (b, right) Electronic states of PtPOP.¹⁶

The lowest excited state in PtPOP has $^3A_{2u}$ symmetry¹³ (Figure 1b). A lifetime of 9.8 μs in deoxygenated water has been reported in previous work,^{14–16} and a quantum yield of $\sim 100\%$ for formation of triplets from upper excited states can be derived from the photophysical data.¹⁶ A total of 52% of the triplets formed deactivate radiatively.^{16,17}

In an early, pioneering paper, Thiel et al.^{18,19} published time-resolved X-ray absorption fine structure (XAFS) spectroscopy measurements on the Pt L_{III} absorption edge of PtPOP with microsecond resolution. The experiment was done on a liquid sheet (72%, w/w, glycerol in H_2O) produced by a jet running at 15 m/s. From the data, a $0.52 \pm 0.13 \text{ \AA}$ inward movement of the P–P planes¹⁸ upon excitation into the $^3A_{2u}$ state was derived.

Under the heading “photocrystallography”,^{20–22} the group of Coppens has pioneered excited-state structure determination in crystals at low temperature by means of TRXRD.²³ As the first excited state ever to be investigated by X-ray diffraction, they determined the Pt–Pt-distance of the $^3A_{2u}$ state of PtPOP in a single crystal of $(\text{Et}_4\text{N})_3\text{HPtPOP}$ at cryogenic temperatures with microsecond time resolution²⁴ and obtained a contraction of 0.28 \AA relative to the ground state. The group of Ozawa²⁵ applied stationary-state methods to reach the value of 0.23 \AA for the same parameter in a single crystal of $(n\text{-Bu}_4\text{N})_2\text{H}_2\text{PtPOP}$ at 54

K. Ohashi et al.²⁶ investigated four different PtPOP salts and obtained average values for the Pt–Pt distance in the steady-state irradiated single crystals.

The diversity of conditions and results in the work quoted above spurred us to strive to determine the $^3A_{2u}$ -state structure of PtPOP in solution at room temperature by TRXRS. The molecule is an attractive target due to its great scattering power, its long lifetime, and its high symmetry, which enhances the effective signal. Furthermore, PtPOP displays a diverse photochemistry in solution,^{9,11} and the work presented here addresses the structure of the reactive state under this condition.

The choice of solvent was based on the following reasoning. Contribution to the signal at small scattering angles (being proportional to the square of the number of coherently scattering electrons) from the positive counterions of the PtPOP salt should be minimized. Thus, four potassium ions (18 electrons each) are preferred over four tetraethylammonium ions (122 electrons each), which contain 29 nuclei each. The potassium salt is not soluble in nonpolar solvents, which confines the selection to water or alcohols as potential media.

Furthermore, current TRXRS experiments require sampling of scattering data from a very high number of excitation cycles, which puts strong demands on the reversibility of the system. The $^3A_{2u}$ state of PtPOP participates in a range of bimolecular photoreactions.^{9–11} It is highly reactive with radical-like properties, abstracting hydrogen atoms from organic compounds. Alcohols such as methanol and glycerol are efficient hydrogen atom donors,²⁷ but PtPOP does not undergo photoreactions in water.

Molecular dynamics (MD) calculations of the solvent response from methanol have been implemented successfully.^{4,5} In contrast, no model has yet described the hydrogen bond force field of water to a satisfactory level. Molecular dynamics simulations of water can sometimes lead to strange results such as formation of layers and clusters. However, as an experimental alternative to MD simulations, it is possible to measure the solvent response in a separate experiment, where the bulk-solvent response to impulse heating is determined in terms of thermodynamic differentials as discussed further below. In terms of data analysis, this approach has been shown to give more accurate results than incorporating MD simulations.²⁸

- (13) More correctly, the $3A_{2u}$ state is split by spin-orbit coupling effects into A_{1u} and doubly degenerate higher E_u components from which phosphorescence is dipole forbidden and allowed, respectively. The spacing is found to be 40–41 cm^{-1} . Brummer, J. G.; Crosby, G. A. *Chem. Phys. Lett.* **1984**, *112*, 15. Shimizu, Y.; Tanaka, Y.; Azumi, T. *J. Phys. Chem.* **1985**, *89*, 1372. At room temperature equilibrium is rapidly established, and for the present purpose the components can be treated as one.
- (14) Che, C. M.; Butler, L. G.; Gray, H. B. *J. Am. Chem. Soc.* **1981**, *103*, 7796.
- (15) Peterson, J. R.; Kalyanasundaram, K. *J. Phys. Chem.* **1985**, *89*, 2486.
- (16) Stiegman, A. E.; Rice, S. F.; Gray, H. B.; Miskowski, V. M. *Inorg. Chem.* **1987**, *26*, 1112.
- (17) Heuer, W. B.; Totten, M. D.; Rodman, G. S.; Hebert, E. J.; Tracy, H. J.; Nagle, J. K. *J. Am. Chem. Soc.* **1984**, *106*, 1163.
- (18) Thiel, D. J.; Livins, P.; Stern, E. A.; Lewis, A. *Nature (London, U.K.)* **1993**, *363*, 565.
- (19) Thiel, D. J.; Livins, P.; Stern, E. A.; Lewis, A. *Nature (London, U.K.)* **1993**, *362*, 40.
- (20) Fullagar, W. K.; Wu, G.; Kim, C.; Ribaud, L.; Sagerman, G.; Coppens, P. *J. Synchrotron Radiat.* **2000**, *7*, 229.
- (21) Coppens, P. *NATO Sci. Ser., Ser. C* **1999**, *519*, 275.
- (22) Coppens, P.; Vorontsov, I. I.; Graber, T.; Gembicky, M.; Kovalevsky, A. Y. *Acta Crystallogr., Sect. A: Found. Crystallogr.* **2005**, *A61*, 162.
- (23) Coppens, P. *Chem. Commun.* **2003**, 1317.
- (24) Kim, C. D.; Pillet, S.; Wu, G.; Fullagar, W. K.; Coppens, P. *Acta Crystallogr., Sect. A: Found. Crystallogr.* **2002**, *A58*, 133.
- (25) Ozawa, Y.; Terashima, M.; Mitsumi, M.; Toriumi, K.; Yasuda, N.; Uekusa, H.; Ohashi, Y. *Chem. Lett.* **2003**, *32*, 62.

(26) Yasuda, N.; Uekusa, H.; Ohashi, Y. *Bull. Chem. Soc. Jpn.* **2004**, *77*, 933.

(27) Roundhill, D. M. *J. Am. Chem. Soc.* **1985**, *107*, 4354.

(28) Cammarata, M.; Lorenc, M.; Kim, T. K.; Lee, J. H.; Kong, Q. Y.; Pontecorvo, E.; Lo Russo, M.; Schiro, G.; Cupane, A.; Wulff, M.; Ihee, H. *J. Chem. Phys.* **2006**, *124*, 124504–124504/9.

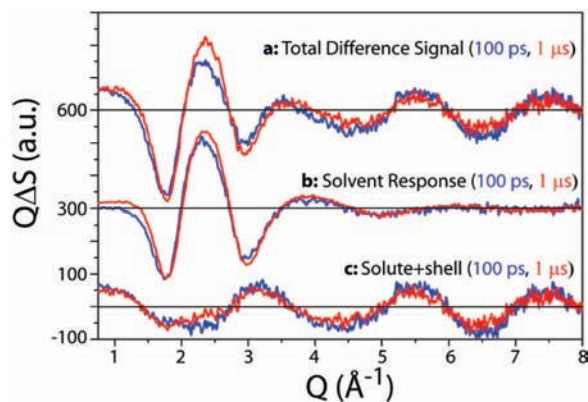


Figure 2. (a, top) Total difference signal, 100 ps (blue) and 1 μ s (red), after optical excitation of 12 mM K_4PtPOP in water obtained by subtracting the average light-on scattering signal from the correspondingly averaged light-off signal. (b, middle) Bulk-solvent difference-signal response as modeled for the two time delays (see the text). (c, bottom) Solute + solvent cage signals obtained by subtracting the bulk-solvent response (b) from the total difference signal (a).

Taking all these aspects into consideration, it was decided to pursue this option and carry out time-resolved X-ray scattering measurements in an aqueous solution of the potassium salt of PtPOP.

Experimental Section

The experiment was performed at the time-resolved beamline ID09B at the European Synchrotron Radiation Facility (ESRF), Grenoble, France. The sample circulated in a liquid jet and was excited using a frequency-tripled femtosecond laser that was phase-locked to the rf clock of the synchrotron. The excitation wavelength was 267 nm, and the pulse was stretched to 2 ps in two SF10 prisms to increase the excitation efficiency. The light-induced structural changes were subsequently probed by high-intensity, polychromatic single X-ray pulses (effective wavelength ~ 0.68 Å, 3% bandwidth, 100 ps long) from the synchrotron isolated by two synchronized choppers. The repetition rate of the pump/probe cycles was 986.3 Hz. A full account of the beamline architecture and instrumentation is provided by Wulff and co-workers²⁹ and in the Supporting Information together with other experimental details.

Results

In TRXRS the *total difference scattering* signal, i.e., the change in X-ray scattering intensity, $\Delta S(q, \tau)$, is measured²⁹ as a function of the scattering vector, $q = (4\pi \sin \theta)/\lambda$, and delay time, τ . The theory of TRXRS^{30–32} describes how the difference signal arises from the changes in electron density of the investigated system and the spatial, temporal, and energetic profiles of the laser/X-ray pulses. Figure 2a displays this difference signal obtained by subtracting the light-off scattering signal from the signal obtained at time delays of 100 ps and 1 μ s, respectively, after optical excitation of 12 mM K_4PtPOP in water.

Contained within this signal are the scattering contributions from every atom–atom pair in the system being affected by optical excitation of PtPOP. To provide a physically sensible description of this response, the atom pairs are separated into

three groups according to the structural changes within (1) the bulk solvent outside the solvation shell (the “solvent-only term”, Figure 2b), (2) the oriented solvent shell around the excited molecule for which the structure is determined by forces between the excited solute and the solvent molecules (the “solute–solvent cross-term”), and (3) the excited PtPOP molecules. In this particular situation, the term “solute” is reserved for this fraction, α , of PtPOP molecules in the excited state since the collective scattering from the remaining fraction ($1 - \alpha$) in the ground state does not manifest itself in the total difference signal. However, according to the experimental procedure, the corresponding response—the solute-only term—is comprised of scattering from the α fraction of excited molecules *minus* the scattering from an equivalent amount α of ground-state molecules at time τ .

Figure 2c is obtained by subtracting the solvent-only term (trace b) from the total difference signal (trace a). Thus, trace c represents the sum of the solute–solvent cross-term (shell) and the solute-only term.

Each contribution to the total difference signal will be described and discussed separately in the following with reference to Figure 2.

Excitation at 267 nm (Figure 1b) transforms PtPOP into the $^1B_{2u}$ excited state ($\epsilon_{\max} = 1550 \text{ M}^{-1} \text{ cm}^{-1}$ at 266 nm). Relaxation into the $^3A_{2u}$ state occurs on a time scale of subpicoseconds with $\sim 100\%$ efficiency.¹⁶ The excess energy³³ from this cascade is dissipated into the solvent. The immediate consequence is a rise in temperature in the solvent surrounding the chromophore. This response equilibrates on a time scale significantly shorter than 100 ps,²⁸ the shortest delay time investigated here. Thus, at 100 ps the bulk solvent surrounding the solute + shell is in a high-temperature, high-pressure configuration from which it relaxes by expansion, a process taking place on time scales from 10 ns to a few hundred nanoseconds.²⁸

Once in the $^3A_{2u}$ state, the excited solute molecules return to the ground state $^1A_{1g}$ on a time scale of microseconds, presumably less than the 9.8 μ s lifetime measured for $^3A_{2u}$ under ideal conditions.¹⁶ A total of 48% of the decay is nonradiative intersystem crossing,^{16,17} and the excess energy is released to the solvent as heat. Obviously, it is too slow to influence the solvent-only scattering signal obtained at 100 ps, but it is important for the signal measured after 1 μ s.

This situation necessitates a fitting procedure for the total difference signals (Figure 2a) in which the time-dependent heating of the solvent (expressed in the temperature rise, ΔT) and solvent expansion (expressed in the variation in density, $\Delta\rho$) go in as fitting parameters together with two structural parameters of the excited PtPOP* molecule. Finally, the excitation ratio, α , that is, the fraction of PtPOP molecules in the excited state at the time of probing, is allowed to vary as the fifth fitting parameter. The whole procedure is explained in detail below.

First, the solvent-only term is addressed following the method of Cammarata et al.²⁸ The bulk-solvent contribution to the scattering signal at all time delays is described by a linear combination of two thermodynamic differentials, i.e., $\Delta S_{\text{solvent}} = \Delta T(\partial\Delta S/\partial T)_\rho + \Delta\rho(\partial\Delta S/\partial\rho)_T$, where ΔT (K) is the temperature change and $\Delta\rho$ (kg/m^3) the density change. The differentials were determined in independent experiments by

(29) Wulff, M.; Plech, A.; Eybert, L.; Randler, R.; Schotte, F.; Anfinrud, P. *Faraday Discuss.* **2002**, *122*, 13.

(30) Bratos, S.; Mirloup, F.; Vuilleumier, R.; Wulff, M. *J. Chem. Phys.* **2002**, *116*, 10615.

(31) Bratos, S.; Mirloup, F.; Vuilleumier, R.; Wulff, M.; Plech, A. *Chem. Phys.* **2004**, *304*, 245.

(32) Henriksen, N. E.; Moller, K. B. *J. Phys. Chem. B* **2008**, *112*, 558.

(33) This amounts to 49% of the absorbed photonic energy on the basis of the 0–0 vibronic transition observed at 540 nm in the phosphorescence spectrum in the crystalline state at 10 K: Rice, S. F.; Gray, H. B. *J. Am. Chem. Soc.* **1983**, *105*, 4571.

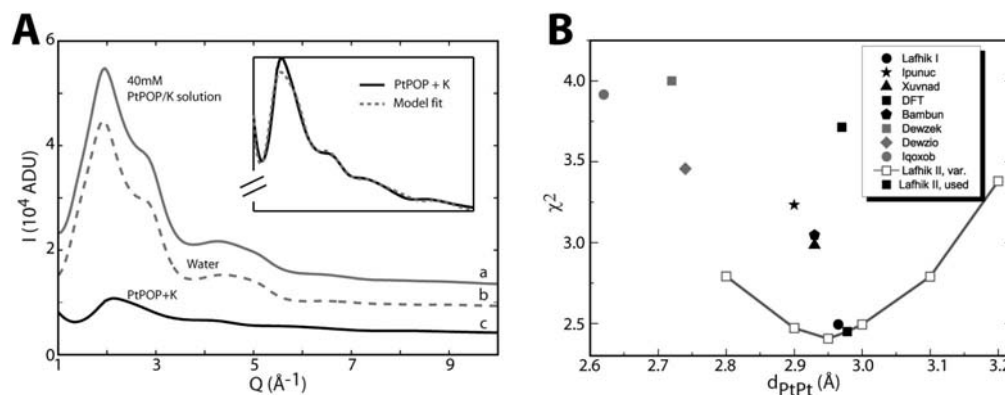


Figure 3. (A) Monochromatic steady-state scattering intensity profiles for a capillary filled with a 40 mM K_4PtPOP /water solution (trace a) and for a capillary filled with pure water (trace b). The difference (trace c) represents the enhanced scattering due to the dissolved ions. The inset shows this signal (enlarged) and a simulated scattering profile for the structural model that produces the best fit to the data with scaling constants $c_1 = 0.25$, $c_2 = 6.1$, and $c_3 = 0.045$. The ratio c_1/c_2 is considerably larger than what would be expected from stoichiometric considerations (1/4). The discrepancy is tentatively attributed to increased low- Q scattering due to solvation shells and/or nonidentical capillary tubes. (B) Reduced χ^2 values for all the tested structures labeled by their six-letter CCDC code and arranged according to the distance between the two Pt atoms: Gray, filled markers correspond to PtPOP structures obtained from X_2PtPOP crystal structures, where X corresponds to halogen atoms (Cl, Br, or I) being subsequently removed from the structure for this analysis. The single DFT structure included is the B88LYP/FC-ZORA structure presented by Novozhilova et al.³⁸ Best fits (lowest χ^2) are found for structures with Pt–Pt distances around 2.95–3.0 Å. For the best fit structure (Lafhik II) the PtPt ground-state distance was further varied to assess whether even longer PtPt distances would produce a better fit, which was not the case (Lafhik II, var.).

submitting a sample of pure water to short NIR pulses. Further details are provided in the Supporting Information. The solvent-only contributions displayed in Figure 2b represent the final ΔT and $\Delta\rho$ values reached after global fitting of the $\Delta S(q, \tau)$ signals in trace a. It is noticed that contributions from the solvent-only term dominate the region below $Q = 4 \text{ \AA}^{-1}$.

In any liquid solution the solvent molecules around every single solute molecule are more or less oriented in accordance with the shape and electron distribution of the solute and the intermolecular forces between them. The PtPOP ion carries four negative charges, and the interactive forces between it and the water molecules are strong and composed of dipolar as well as dispersive terms. A dynamic aspect of optical excitation in liquids is relaxation of the solvent molecules around the excited solute molecule in response to the altered charge distribution and geometry. The process occurs on a time scale of picoseconds, after which the contribution to the TRXRS signal (termed the solute–solvent cross-term) is constant within the lifetime of the excited species.

Excitation of PtPOP to the lowest excited states ($^1,^3A_{2u}$) implies a shift of an electron from an external axial orbital ($d\sigma^*$) to a bonding orbital ($p\sigma$) between the Pt atoms. The excitation results in hole formation on a metal center at an open coordination site.¹⁰ Since no solvatochromism is observed,¹⁵ it can be concluded that there is no axial coordination of solvent molecules either in the ground or in the excited $^3A_{2u}$ states. The contribution from the solute–solvent cross-term of the solvation shell to the difference signal is thus expected to be negligible. Accordingly, the difference signals (Figure 2c) obtained by subtracting the bulk-solvent responses (trace b) from the raw signals (trace a) represent the difference scattering signals which are due to fractional excitation of the PtPOP molecules—the solute-only term.

The X-ray light-on scattering signal differs from the light-off signal, not only due to the altered molecular form factor of the excited state but also because the number of ground-state molecules is lower. The next step in resolving the time-dependent difference scattering signal is to calculate the molecular form factors of PtPOP in both the ground state and excited triplet state. Usually such calculations are based on

structures obtained from crystallographic data or computations.^{24,34,35} The present case calls for caution, however, since there is no way to ensure that molecular structures in solution are the same as in the crystal,³⁶ and there is no kind of alternative experimental data which can provide exact structures either of the ground or of the excited state.³⁷ Furthermore, calculations with nuclei so heavy as platinum are complicated due to relativistic effects³⁸ although the difficulties have been reduced by recent advances.³⁹

To reach structures and associated molecular form factors necessary for interpretation of the time-resolved data, the steady-state scattering signal of aqueous PtPOP solutions with concentrations from 5 to 40 mM in a Lindemann capillary was recorded using 26 keV monochromatic X-rays. It was found that the integrated radial profiles for several different concentrations of PtPOP scaled linearly with concentration, from which it was concluded that no ground-state association of PtPOP occurs in this concentration range (data not shown). Figure 3A, trace a, shows one such radial profile for a PtPOP concentration of 40 mM. To assess the ground-state structure of PtPOP in aqueous solution, a procedure analogous to the one employed by Kong et al. in their high-resolution, 88 keV study of 1,2-diiodoethane in solution³⁴ was employed with the 26 keV steady-state data as described in further detail below.

The steady-state signal from pure water (Figure 3A, trace b) was obtained independently under identical conditions and

(34) Kong, Q.; Kim, J.; Lorenc, M.; Kim, T. K.; Ihee, H.; Wulff, M. J. *Phys. Chem.* **2005**, *109*, 10451.

(35) Techert, S.; Schotte, F.; Wulff, M. *Phys. Rev. Lett.* **2001**, *86*, 2030.

(36) Maliarik, M.; Nagle, J. K.; Ilyukhin, A.; Murashova, E.; Mink, J.; Skripkin, M.; Glaser, O. J.; Kovacs, M.; Horvath, A. *Inorg. Chem.* **2007**, *46*, 4642.

(37) Calculations based on spectroscopic data rely on Badger's rule, which implies knowledge of the binding force constant: Che, C. M.; Butler, L. G.; Gray, H. B.; Crooks, R. M.; Woodruff, W. H. *J. Am. Chem. Soc.* **1983**, *105*, 5492. Badger, R. M. *J. Chem. Phys.* **1935**, *3*, 710. Stein, P.; Dickson, M. K.; Roundhill, D. M. *J. Am. Chem. Soc.* **1983**, *105*, 3489.

(38) Novozhilova, I. V.; Volkov, A. V.; Coppens, P. *J. Am. Chem. Soc.* **2003**, *125*, 1079.

(39) Pierloot, K.; van Besien, E.; van Lenthe, E.; Baerends, E. J. *J. Chem. Phys.* **2007**, *126*, 194311–194311/8.

subtracted, resulting in Figure 3A, trace c, which shows the combined contributions from the ions (PtPOP⁴⁻ and K⁺) and their solvent shells (cross-term).

To reach a representative structure for the X-ray scattering signal of the PtPOP ground state in solution, a number of structures obtained in XRD studies of PtPOP crystals and a DFT-based calculation were taken into account. The Pt–Pt distance in the crystal data^{24,26} obtained from the Cambridge Crystallographic Centre database spans the range from 2.9126 to 2.979 Å. A range of DFT-based computational methods have been applied to PtPOP, producing Pt–Pt distances from 2.837 to 3.04 Å.^{40,41} Among these, the one based on the B88LYP functional applying the FC/ZORA approximations was selected and included in the procedure.³⁸

For each of these structures the scattering intensity was calculated using the Debye formula for orientational averaging:

$$I(Q) \propto F_{\text{mol}}^2 = \sum_{i < j} f_i f_j \frac{\sin(Qr_{ij})}{Qr_{ij}} + f_{kk}^2, \quad f_{i,j,k} = f(Q) = \sum_{j=1}^4 a_j e^{-b_j(Q/4\pi)} + c$$

where the a , b , and c coefficients in the latter expression are the tabulated Cromer–Mann parameters.⁴² The contribution from Compton scattering was also calculated from tabulated parameters and included in the intensity calculation. The calculated intensity profile ($S_{\text{PtPOP}}(Q)$) was combined with the contribution from the K ions ($S_{\text{K}}(Q)$), a background signal (S_{bg}), and a remanent water signal ($S_{\text{H}_2\text{O}}(Q)$) through the expression $S_{\text{fit}}(Q) = c_1 S_{\text{PtPOP}}(Q) + c_2 S_{\text{K}}(Q) + c_3 S_{\text{H}_2\text{O}}(Q) + S_{\text{bg}}$ and fitted to the data (Figure 3A, trace c) with the scaling parameters c_1 , c_2 , and c_3 . The water signal was introduced into the fitting procedure to compensate for slight differences in capillary size, resulting in significantly improved fits.

The quality of the fit was parametrized through the expression $\chi^2 = \sum_Q (S_{\text{data}}(Q) - S_{\text{fit}}(Q))^2 / S_{\text{data}}(Q)$, assuming the standard deviation of the data at any Q point to be the square root of the number of counts at that point.

The right panel of Figure 3 shows the χ^2 values obtained by applying the scattering intensity calculation and the fitting procedure to the crystal and DFT-calculated structures. A clear trend in the data is evident as structures with Pt–Pt separations around 2.95–3.0 Å fit the experimental scattering curve better than all other structures in contrast with recent results for (Bu₄N)₄PtPOP in ethanol solution,⁴³ where analysis of EXAFS data is reported to give a Pt–Pt separation of 2.876 Å. Furthermore, the ground-state PtPt distance for the best fit structure (Lafhik II) was varied from 2.8 to 3.2 Å to check whether extended PtPt distances would lead to better fits. As Figure 3B shows, this was not the case. Our analysis leads to a Pt–Pt distance close to 2.98 Å as the best estimate for PtPOP in solution in the ground state. The corresponding overall structure (Lafhik II benzyltriethylammonium-PtPOP at 103 K)²⁶ was applied in the following analysis of the time-resolved data.

Due to the random orientational distribution of molecules in a liquid, X-ray scattering data from complex molecules in solution do not allow a direct ab initio structural determination. However, information about key structural parameters can be obtained by fitting a simulated difference signal, ΔS , calculated for a range of hypothetical structures of the transient state to the experimentally determined $\Delta S(Q)$ curves and evaluating the quality of the fit.⁴ In the present case the key parameters are the Pt–Pt distance and the distance between the P planes.

The starting point for the structural variation study was the ground state obtained as described above, and the structural parameter was determined according to a maximum-likelihood analysis⁴⁴ based on a reduced χ^2 estimator as described below. The Pt–Pt distance in PtPOP* was varied from 2.50 to 3.0 Å in steps of 0.02 Å. For each, the change in the Pt–P bond length was parametrized through changing the distance between the phosphorus planes from 2.50 to 3.30 Å in 0.02 Å steps along the Pt–Pt axis. The initial distance between the planes in the ground-state structure was 2.92 Å. For each structure, uniquely determined by the two structural parameters, the difference scattering pattern relative to the ground state was calculated using the Debye expression introduced above and incorporating the polychromaticity of the beam by calculating an intensity-weighted average of the contribution from individual wavelengths in steps of 0.2 keV from 13 to 19 keV.

Thus, a total of 1066 structures were probed, and in each case, the photoexcitation fraction, α , was varied as a free third parameter until the best fit was obtained. Concomitantly, the bulk-solvent response was fitted by varying ΔT and $\Delta\rho$ in $\Delta S_{\text{solvent,bulk}} = \Delta T(\partial\Delta S/\partial T)|_p + \Delta\rho(\partial\Delta S/\partial\rho)|_T$ as described above and in the Supporting Information.

For each set of the five fitting parameters, the quality of the fit was determined through evaluation of a reduced χ^2 estimator with χ^2 given by

$$\chi^2(d_{\text{PtPt}}, d_{\text{PpPp}}, \alpha, \Delta T, \Delta\rho) = \sum_Q \frac{(S_{\text{fit}}(Q) - S_{\text{exp}}(Q))^2}{2\sigma(Q)^2} / (N - p - 1)$$

where $\sigma(Q)$ is the standard deviation evaluated at each Q point, N is the number of Q points, and p is the number of free parameters in the fit. These are (1) d_{PtPt} , the Pt–Pt distance in the ³A_{2u} state, (2) d_{PpPp} , the distance between the P planes in the ³A_{2u} state, the excitation fraction α , and the two thermodynamic parameters ΔT and $\Delta\rho$.

Assuming initially no knowledge of the two thermodynamic variables ΔT and $\Delta\rho$, the 5-dimensional likelihood space spanned by d_{PtPt} , d_{PpPp} , α , ΔT , and $\Delta\rho$ can be projected into the 3-dimensional subspace spanned by d_{PtPt} , d_{PpPp} , and α for a direct representation of the correlations between the structural parameters only.

Figure 4 illustrates the correlations and uncertainties related to the determination of the model parameters from the data set obtained with a 100 ps delay. Plots of the three-parameter likelihood distribution function $\exp(-\chi^2)$ are projected onto the planes bounding this subset of parameter space and spanned by each set of two parameters (panel A–C contours contain 68%, 95%, and 99.7% of the likelihood distribution, respectively) as well as onto the distance axis related to the structural parameters (panel D). Panel A clearly shows the strong correlation between the determination of d_{PtPt} and α , with a small

(40) Novozhilova, I. V.; Volkov, A. V.; Coppens, P. *Inorg. Chem.* **2004**, *43*, 2299.

(41) Stoyanov, S. R.; Villegas, J. M.; Rillema, D. P. *J. Phys. Chem. B* **2004**, *108*, 12175.

(42) Wilson, A. J. C. *International Tables of Crystallography*; Kluwer Academic Publishers: Dordrecht, The Netherlands, 1992; Vol. C, pp 193–502.

(43) van der Veen, R. M.; Milne, C. J.; Pham, V. T.; El Nahhas, A.; Weinstein, J. A.; Best, J.; Borca, C. N.; Bressler, C.; Chergui, M. *Chimia* **2008**, *62*, 287.

(44) Press, W. H.; Flannery, B. P.; Teukolsky, T. A.; Vetterling, W. T. *Numerical Recipes—The Art of Scientific Computing*; Cambridge University Press: Cambridge, U.K., 1986.

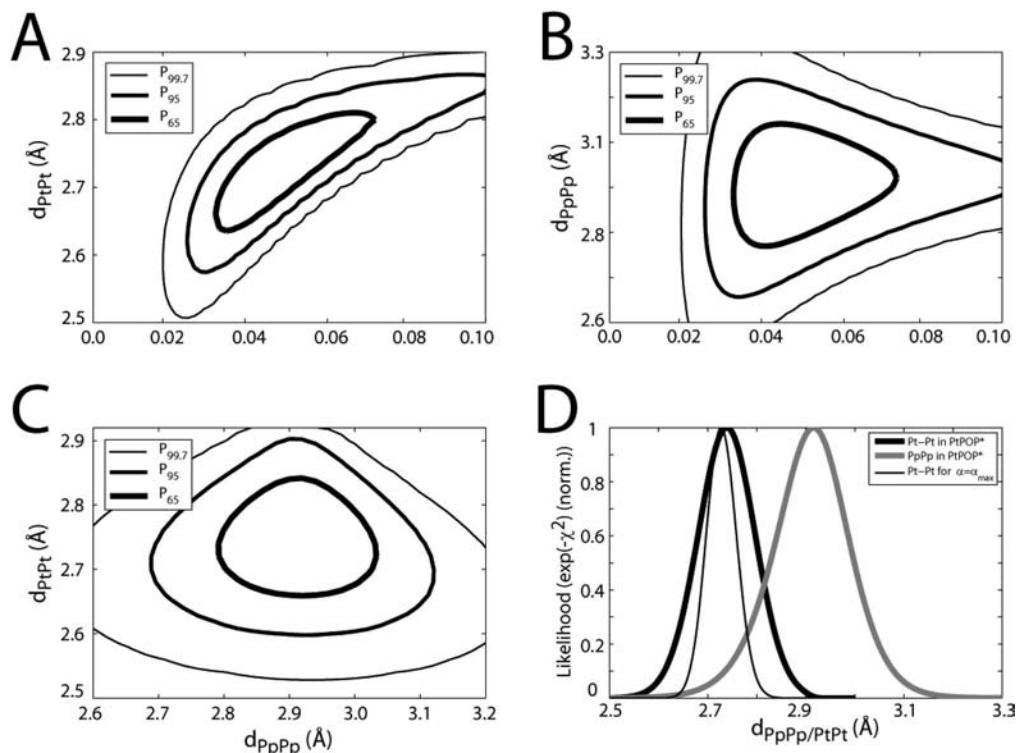


Figure 4. Fitting of the data set obtained at a 100 ps delay. Panels A–C show the three-parameter likelihood distribution function $\exp(-\chi^2)$ projected onto the three planes bounding the subset of parameter space spanned by the excitation fraction, α , and the two structural parameters d_{PpPp} and d_{PtPt} . The contours enclose 68%, 95%, and 99.7% of the probability distribution, respectively. Clear correlation is seen between the determination of d_{PtPt} and α , but only weak or no correlation appears between the other pairs of parameters, as also observed for correlations with the hydrodynamic variables ΔT and $\Delta\rho$ (not shown). The curves in panel D represent the (normalized) projections onto the d_{PtPt} (black) and d_{PpPp} (gray) axes. From the width of these distributions the uncertainty related to the parameter determination can be estimated. The thin black line in panel D shows the distribution function for d_{PtPt} if the excitation fraction is restricted to the best fit value $\alpha = 4.2\%$ (see the text). The contours in panels A–C are wavy due to the finite step size of the parameter variation.

d_{PtPt} in the excited state necessitating a large fraction of excited-state molecules to account for the observed difference signal. Only weak correlation between the other parameters is observed. Panel D shows the projection of the likelihood distribution onto the d_{PtPt} and d_{PpPp} axes, respectively. From these distributions the key structural parameters are determined to be $d_{\text{PtPt}} = 2.72 \pm 0.06 \text{ \AA}$ and $d_{\text{PpPp}} = 2.92 \pm 0.08 \text{ \AA}$. As also noticed by Kim et al.,²⁴ the significant uncertainty in the determination of d_{PtPt} is related to the uncertainty in the fraction of excited-state molecules. The thin black line in panel D illustrates the shape of the d_{PtPt} distribution function if α is fixed to the value 4.2% for which the best fit is obtained. It is clearly seen how independent experimental determination of this parameter is crucial for minimizing the uncertainties related to the determination of structural parameters in this type of investigation.⁴⁵

For the 1 μs data set, the shapes of the likelihood distributions are identical to those presented in Figure 4 and the corresponding structural parameters obtained almost identical: $d_{\text{PtPt}} = 2.78 \pm 0.08 \text{ \AA}$ and $d_{\text{PpPp}} = 2.93 \pm 0.08 \text{ \AA}$. However, the photoexcitation fraction $\alpha = 3.2\%$ is lower, corresponding to an average lifetime of ca. 3.7 μs .

The best fit values obtained for the free parameters ΔT and $\Delta\rho$ are for the 100 ps data set $\Delta T = 0.23 \pm 0.04 \text{ K}$ and $\Delta\rho = 0.05 \pm 0.03 \text{ g cm}^{-3}$. Corresponding values for the 1 μs data set are $\Delta T =$

$0.32 \pm 0.04 \text{ K}$ and $\Delta\rho = -0.03 \pm 0.03 \text{ g cm}^{-3}$. The temperature rise is somewhat higher than expected from the excitation ratio, α , which indicates the presence of nonlinear multiphoton processes such as re-excitation of $^1A_{2u}$ and $^3A_{2u}$. The $\Delta\rho$ values are close to the uncertainties and cannot be commented on.

As demonstrated in the Supporting Information, another means of narrowing the uncertainty of the determination is to incorporate all data obtained at all time delays. Doing so, the same numerical values for the two structural parameters are obtained, but the precision is considerably improved to $\pm 0.03 \text{ \AA}$ for d_{PtPt} and to $\pm 0.04 \text{ \AA}$ for d_{PpPp} .

Figure 5 illustrates how the global best fits correspond to excited-state structures for which the scattering signals are calculated as the black lines. The agreement with the experimental points is rather satisfactory. The quality of the fits validates the assumption that no significant structural changes occur in the solvent shell due to the optical excitation of PtPOP (the solute–solvent cross-term). The 100 ps data set is considered the best due to the better signal-to-noise ratio. The corresponding Pt–Pt distance is 2.74 \AA , the distance between the phosphorus planes is 2.92 \AA , and the excitation fraction is 4.2% for this best fit model.

Discussion and Summary

The experiments described represent the first successful structural characterization of an electronically excited polyatomic molecule in solution by means of X-ray scattering.⁴⁶ Furthermore, the $^3A_{2u}$ state of PtPOP is also the largest and structurally most complicated transient species investigated by this technique. As a decisive step in the data processing procedures the time-resolved response from

(45) Estimating the fraction of excited states present at the time of probing is not a straightforward matter in the present case. At the level of intensity employed several nonlinear processes are bound to occur, e.g., two-photon excitation, stimulated emission, and triplet–triplet annihilation. The experimental parameters were varied to obtain the strongest scattering signal at the sacrifice of the knowledge of α .

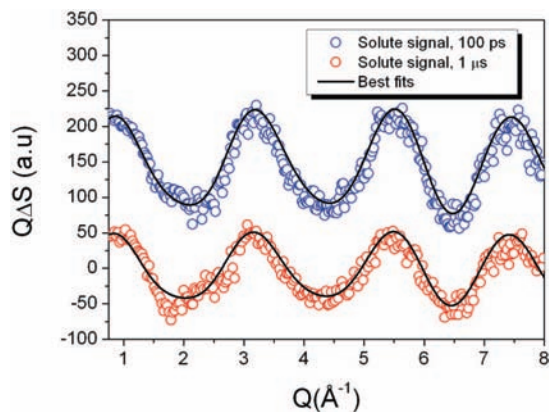


Figure 5. Solute-only contributions to the difference signal at 100 ps delay (blue circles, offset) and 1 μ s delay (red circles) and the best fit simulated scattering signals (black lines) from the models that produce the best fit to the total difference signal (Figure 2a). For both the simulated signals and the data, the bulk-solvent contribution, determined through the global maximum-likelihood analysis, has been subtracted to emphasize the contribution to the difference scattering signal from changes in the molecular structure of the solute. Note the decrease in oscillation amplitude, corresponding to the lower population of excited-state PtPOP at 1 μ s.

the solvent (water) was based on an independent experiment involving NIR excitation from which a set of thermodynamic differentials were obtained.

The primary structural parameter in the $^3A_{2u}$ state is the Pt–Pt distance for which a value of 2.74 ± 0.06 Å was obtained. It represents a contraction of 0.24 Å or 8% from the ground-state Pt–Pt distance (2.98 Å; see above).

As the second parameter to be measured, the distance between the P planes in the excited state was determined to be 2.92 ± 0.08 Å, which—within the experimental accuracy—is identical to the ground-state distance. This result implies that a slight lengthening of the Pt–P bond occurs following excitation.

The Pt–Pt and Pt–P distances in the ground-state PtPOP ion (potassium salt) in the crystal are 2.925 and 2.320 Å, respectively.¹² In a time-resolved diffraction study with synchrotron radiation at 17 K Coppens and co-workers^{23,24} found the Pt–Pt distance to contract by 0.28 Å (to 2.64 Å) upon excitation to $^3A_{2u}$. It is interesting that a 0.1 Å longer Pt–Pt distance is obtained in the present work. The difference could reflect the constraints of the crystal lattice at cryogenic temperatures in which the identity of the cations (in casu three tetraethylammonium ions and one proton) can play a decisive role. Thus, it should be noted that the ground-state Pt–Pt separation in these two crystal-based studies is significantly shorter (2.913 Å) than the one adopted here (2.975 Å), suggesting confinement effects due to intermolecular interac-

tions in the crystals.^{26,36} It should also be recognized that the sublevels of the $^3A_{2u}$ state are frozen out at 17 K.

The Pt–Pt vibrational frequency in the ground and excited triplet states is another parameter which reflects the bond strength. Values of 110 and 155 cm^{-1} , respectively, were obtained from the vibronic fine structure in the optical spectra at 10 K of the barium salt, clearly reflecting a stronger Pt–Pt bond in the upper state. Rice et al.⁴⁷ undertook a Franck–Condon analysis of the spectra and calculated a Pt–Pt distance of 2.71 Å in the $^3A_{2u}$ state.

In aqueous solution at room temperature, time-resolved resonance Raman spectroscopy presented by Gray and co-workers⁴⁸ has provided Pt–Pt stretching frequencies of 118 cm^{-1} for the $^1A_{1g}$ state and 156 cm^{-1} for the $^3A_{2u}$ state. These values indicate that the Pt–Pt bonding force constant in the $^3A_{2u}$ state is not strongly affected by the crystal lattice. When the solution frequencies were subjected to a calculation according to Badger's rule,⁴⁹ the result was a finding of 2.75 Å for the excited-state Pt–Pt separation.⁵⁰ The accordance with the value obtained in the present work under identical physical conditions is satisfying.

However, this agreement might be coincidental as Badger's rule is inaccurate³⁷ and the absolute value of the Pt–Pt distance in PtPOP* determined in the present work relies on the ground-state solution geometry which has been reached in a semiexperimental manner based on steady-state X-ray scattering data (Figure 3A), crystal data, and computations (Figure 3B). While it seems verified that the Pt–Pt distances in both the ground and excited states are longer in solution than in the crystal, they are linked together. Therefore, the pertinent parameter to consider when solution data and crystal data are compared is the contraction. When the value obtained here is compared with the crystal data quoted above^{24,25} and the standard deviations are considered, the difference between Pt–Pt bond contraction upon excitation in solution and in the crystalline state is not significant.

Thiel et al.^{18,19} applied XAFS to obtain an inward movement of the P–P-planes of 0.52 ± 0.13 Å in a time-resolved study on glycol/water solutions at room temperature. Since this value is roughly twice that of other estimates, the discrepancy might rely on a misinterpretation of the geometry.

DFT calculations on the PtPOP ion in vacuum and in water lead to Pt–Pt distances, in agreement with the crystallographic and spectroscopic results cited above.^{38,41,51}

The $^3A_{2u}$ state of PtPOP is only a single representative of a group of similar molecular states among bi- and polynuclear metal complexes which can be investigated in solution by time-resolved X-ray diffractive methods. A TRXRS investigation of exciplex formation between PtPOP and Ti^+ will be described in a forthcoming paper.

Acknowledgment. The help provided by E. Pontecorvo and F. Ewald at the ID09B beamline is very much appreciated. This work was made possible through support from the Danish National Science Foundation's Centre for Molecular Movies. Financial support from DANSCATT is gratefully acknowledged.

Supporting Information Available: Synthesis of PtPOP, experimental details, absorption and emission spectra, experimental setup at beamline ID09B (ESRF, Grenoble), data reduction, calculations of the molecular form factors for the ground state and excited triplet state of PtPOP, simulation of the solvent-only term by linear combination of thermodynamic differentials, and global treatment of scattering data from all time delays. This information is available free of charge via the Internet at <http://pubs.acs.org>.

JA804485D

- (46) The A/A' state of I_2 qualifies as the first excited diatomic molecular state being investigated by TRXRS: Wulff, M.; Bratos, S.; Plech, A.; Vuilleumier, R.; Mirloup, F.; Lorenc, M.; Kong, Q.; Ihee, H. *J. Chem. Phys.* **2006**, *124*, 34501. However, the majority of the excited-state population was formed as a product of recombination of iodine atoms. In the present work the $^3A_{2u}$ state of PtPOP was populated by optical excitation.
- (47) Rice, S. F.; Gray, H. B. *J. Am. Chem. Soc.* **1983**, *105*, 4571.
- (48) Che, C. M.; Butler, L. G.; Gray, H. B.; Crooks, R. M.; Woodruff, W. H. *J. Am. Chem. Soc.* **1983**, *105*, 5492.
- (49) Badger, R. M. *J. Chem. Phys.* **1935**, *3*, 710.
- (50) Stein, P.; Dickson, M. K.; Roundhill, D. M. *J. Am. Chem. Soc.* **1983**, *105*, 3489.
- (51) Pan, Q. J.; Fu, H. G.; Yu, H. T.; Zhang, H. X. *Inorg. Chem.* **2006**, *45*, 8729.